Mobility *vs* Alignment of a Semiconducting π-Extended Discotic Liquid-crystalline Triindole

Constanza Ruiz[1,2], Upendra K. Pandey,[3,4], Roberto Termine[3], Eva María García-Frutos,[1] Guzmán López-Espejo,[5] Rocío Ponce Ortiz,[5] Wei Huang,[2] Tobin J. Marks[2], Antonio Facchetti,[2] M. Carmen Ruiz Delgado,[5] Attilio Golemme,[3] Berta Gómez-Lor[1]*

1 Instituto de Ciencia de Materiales de Madrid, CSIC, Cantoblanco, 28049, Madrid, Spain

2 Department of Chemistry and the Materials Research Center, the Argonne-Northwestern Solar Energy Research Center, Northwestern University, 2145 Sheridan Road, Evanston, Illinois 60208, United States

3 LASCAMM CR-INSTM, CNR-NANOTEC Lab LiCryL, Dipartimento di Fisica, Università della Calabria, 87036 Rende, Italy

4 Interdisciplinary Centre for Energy Research, Indian Institute of Science, Bangalore, 560012, India

5 Department of Physical Chemistry, University of Málaga, 29071, Málaga, Spain

Keywords. Organic semiconductors, discotic liquid-crystals, OFETS, SCLC measurements, hole mobility.

Abstract

The *p*-type semiconducting properties of a triphenylene-fused triindole mesogen, have been studied by applying two complementary methods which have different alignment requirements. The attachment of only three flexible alkyl chains to the nitrogen atoms of this π-extended core is sufficient to induce columnar mesomorphism. High hole mobility values (0.65 $cm^2V^{-1}s^{-1}$) have been estimated by space-charge limited current (SCLC) measurements in a diode-like structure which are easily prepared from the melt, rendering this material a good candidate for OPVs and OLEDs devices. The mobility predicted theoretically via a hole-hopping mechanism is in very good agreement with the experimental values determined at the SCLC regime. On the other hand the hole mobility determined on solution processed thin film transistors (OFETs) is significantly lower, which can be rationalized by the high tendency of these large molecules to align on surfaces with their extended π-conjugated core parallel to the substrate as demonstrated by SERS. Despite the differences obtained with the two methods, the acceptable performance found on OFETs fabricated by simple drop-casting processing of such an enlarged aromatic core is remarkable and suggest facile hopping between neighboring molecular columns owing to the large conducting/isolating ratio found in this discotic compound.

Introduction

The field of organic electronics has evolved impressively in the last few years and the first device generation based on organic semiconductors has reached the market.[1,2] The major contribution advancing this field have been associated to the development of organic

semiconductors exhibiting high charge carrier mobility. However finding organic semiconductors with the proper balance between mobility and processability, remains challenging. In this context discotic liquid crystals, constituted by an aromatic central core surrounded by flexible alkyl tails, are among the most promising candidates.[3-5] In the columnar mesophases induced by discotic mesogens the aromatic cores are strongly interacting ensuring an uniaxial pathway for efficient charge carrier transport while the soft and self-repairing nature of these materials facilitates their easy processing and the realization of defect free domains over large areas.[6-10] Due to their characteristic molecular structure consisting of a π-conjugated conducting core surrounded by electrically insulating substituents, charge transport in discotic liquid crystals is highly anisotropic and a precise control of the orientation of the columnar axis on the substrate is therefore imperative to enable optimal charge transport.[11, 12]

This high dependence of the electrical performance on the degree of columnar alignment represents a serious drawback for application of discotic mesogens in several opto-electronic devices by simple solution-processing techniques. Although the uniform macroscopic orientation of columns on different substrates has been successfully achieved via different strategies such as the application of electric[13,14] or magnetic fields[12,15], use of surface modifiers[16,17], and confinement effects[18,19] among others, to date solutions vary from material to material and are complicated by the fact that each type of device has different geometry requirements. Planar alignment of columns (conducting channel parallel to the dielectric substrate) is needed in thin-film transistors, whereas homeotropic alignment of columns (conducting channel perpendicular to the electrodes) is required in photovoltaic cells or light-emitting diodes.[7,8] At this stage, the controlled alignment of columns represents a major challenge for the practical application of discotic liquid crystals.

Heptacyclic 10,15-dihydro-5*H*-diindolo[3,2-*a*:3',2'-*c*]carbazole (triindole) has been widely studied as a π-conjugated platform in the construction of high mobility semiconducting liquid crystals.[20-23] Especially remarkable is the record hole mobility values determined on hexaphenyltriindole columnar mesophases (up to 2.8 $cm^2V^{-1}s^{-1}$)[21] as a result of the favorable synergy between the intrinsic properties of the platform and the high degree of supramolecular order triggered by the bulky phenyl moieties that efficiently interlock the molecules within the columns. Interestingly, three-fold oxidative cyclodehydrogenation of hexaphenyltriindole render a significantly enlarged aromatic core, with structural characteristics of both triphenylene moieties and triindole. In this π-extended discotic core, the attachment of only three flexible alkyl chains to the nitrogen atoms is sufficient to induce mesomorphism.[24] Thus compound **1** (Figure 1) functionalized with six peripheral methyl groups and three long flexible dodecyl chains attached to the nitrogens shows an ordered mesophase in a broad range of temperatures. In this compound the ratio of conducting versus isolating fraction is considerably enhanced compared to triindole liquid crystals not only by enlarging the size of the central core but also by reducing the amount of isolating peripheral chains.

In this manuscript we investigate the semiconducting properties of this aromatic platform with the aim of lowering the dependence of alignment usually found on discotic liquid crystals. Particularly, we explored the electrical properties of compound **1** via two complementary methods: space-charge limited current (SCLC) measurements in a diode-like structure[25-29] and field effect mobility measurements in a thin-film transistor device[30, 31] which could be easily prepared by melt and solution processing, respectively. A hole mobility of 0.64 $cm^2V^{-1}s^{-1}$ could be determined by SCLC method which is among the highest recorded for a hole-mobility liquid crystal.[32] Measured field effect mobility values are 3 order of magnitude lower, which can be

ascribed to the different alignment requirements for both techniques. Despite the differences in mobilities obtained with the two methods, the acceptable performance found on **1**-based OFET$_S$ fabricated by simple drop-casting processing of such an enlarged aromatic core is remarkable and suggest that an increase of the dimensionality of the charge carrier pathway have been achieved in this system as a result of the large conducting/isolating ratio found in this discotic compound.

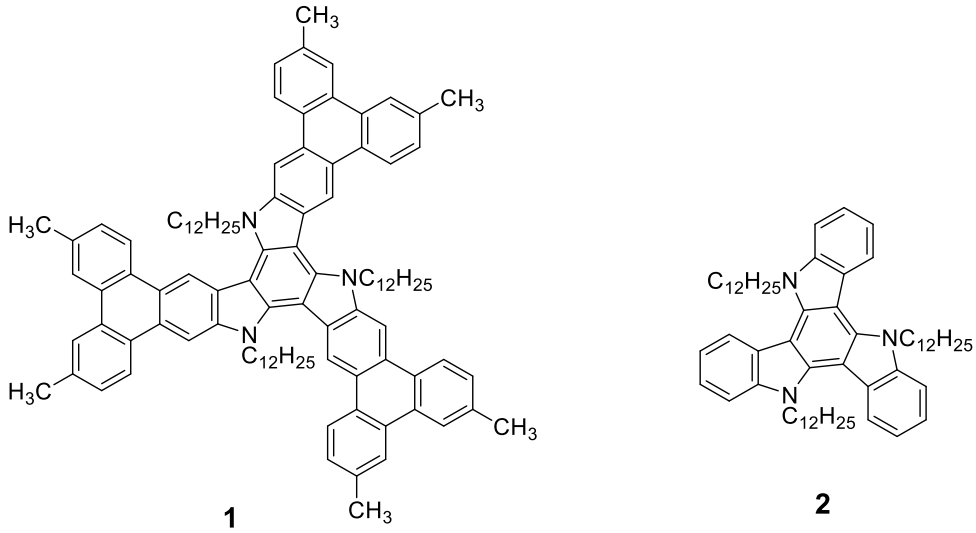

Figure 1: Structure of triphenylene-fused triindole **1** and triindole **2** cores under study.

Experimental Section

Raman measurements. Microscope Raman scattering spectra with excitation at λ = 785 nm were performed on Laser-Raman spectrophotometer (NRS-5100 JASCO). The operating power for the exciting laser radiation was kept to 12.2 mW in all experiments. Samples were analyzed as bulk or thin films by averaging 50 scans with 10 s of integration time. The thin films samples prepared by spin-coating or drop-casting solutions were deposited on Au or SiO_2 surfaces.

Space Charge Limited Current (SCLC) measurements. Cells for mobility measurements consisted of two glass substrates with different electrodes. One substrate had several ITO stripes with a 1 mm width, obtained via photolithography from uniformly ITO coated commercial glass (UNAXIS, 110 nm ITO thickness). These substrate were cleaned by ultra-sonication, using a sequence of lightly soapy water, distilled water, acetone and isopropyl alcohol. The clean glasses were then dried overnight at 90 °C in a vacuum oven before being transferred to a glove box with a nitrogen atmosphere (O_2 < 0.1 ppm, H_2O < 0.1 ppm). Glass substrates with gold electrodes were instead prepared by thermal evaporation of gold on glass substrates cleaned as described above. Cells were prepared by squeezing the melt at 150 °C between two substrates with patterned electrodes, gold on one side and ITO on the other side. After cooling to room temperature, samples were sealed with epoxy glue. Both thickness and SCLC measurements were carried out outside of the glove box. The thickness (typically around 20 micrometers) was obtained by observing the interference in the light transmission in the near-IR region, using an AGILENT 8453 UV-Vis spectrometer. A Keithley 6517A electrometer was used to obtain the Current/Voltage curves, while the capacitance of the cell was measured with an Agilent 4284A LCR meter.

Field-effect transistor fabrication. The characterization of organic field effect transistors was carried out in order to determine field effect charge carrier mobilities (μ_{FET}). In this work, transistors with bottom gate, top contact configuration were used. First, the gate/dielectric substrates (Si/300 nm SiO_2) were cleaned in an ultrasonic bath with acetone, hexane and ethanol previous to drying under a flow of nitrogen. Next, the surface was functionalized with a self-assembled monolayer of hexamethyldisilazane (HMDS) to minimize interfacial trapping sites[33,34]. Then, thin films of compound **1** were made by drop-casting (40µL of a 5mg/ml in

chloroform solution) under nitrogen atmosphere. Finally, 30 nm gold source and drain electrodes were thermal evaporated through a shadow mask. Devices were tested under vacuum by using an Agilent B1500 semiconductor parameter analyzer and a customized vacuum probe station.

Computational details. The theoretical study was carried out in the frame of density functional theory (DFT) using the B3LYP functional[35,36] and the 6-31G** basis set[37,38] as implemented in the Gaussian 09 program.[39] The geometry optimizations of triphenylene-fused triindole **1** and related triindole **2** were performed considering C_3 symmetry constraints. The long dodecyl side chains on the nitrogens of the compounds subjected to the experimental study, were replaced with methyl groups in order to reduce the computational cost. Note that we have recently found that *N*-alkyl substitution of triindoles slightly impacts their electronic properties at the single-molecule level[40]. Based on the resulting ground-state geometries, harmonic vibrational frequencies were calculated analytically at the same theoretical level. The reorganization energies, were calculated directly from the relevant points on the potential energy surfaces using the standard procedure detailed in the literature.[41]

The transfer integrals (electronic couplings) of two adjacent molecules were calculated at the B3LYP/6-31G** level, according to the approach described by Valeev et al.[42] with the corresponding matrix elements evaluated with Gaussian 09. In this approach, the molecular orbitals of the dimer are described using a basis set of localized monomer orbitals. The orbital energies of the dimers are determined by the secular equation **HC**=**SCE**, where **H** is the system Hamiltonian or Fock matrix , **C** is the eigenvector matrix, **S** is the overlap matrix of the monomer molecular orbital basis, and **E** is the diagonal eigenvalue matrix. The electronic coupling can then be calculated directly as the H_{ij} matrix element obtained from the secular equation which is then orthogonalized using Löwdin's symmetric transformation.[42] Note that the

coupling values depend on the functional used and generally increase with the increasing percentage of Hartree-Fock exchange in the functional.[43]

Results and Discussion

The synthesis and mesomorphic properties of compound **1** were previously reported by our group.[24] This compound shows an ordered columnar hexagonal mesophase which extends from 26 ºC to 226 ºC. A lattice constants of a = 24.2 Å has been determined by X-ray diffraction together with a clear 001 diffuse reflection corresponding to the regular stacking of the molecules of 3.85A within the columnar mesophases.[24]

We have performed a Raman spectroscopy comparative study on **1** and the parent *N*-dodecyltriindole **2** in order to investigate the influence of the external triphenylene groups on the π-conjugation. As seen in Figure 2 a good agreement is found between the theoretical and the experimental Raman spectra. The Raman band associated to a C-C stretching mode (*i.e.*, mode 8a of benzene[44]) localized on the external benzene rings shifts towards higher wavenumbers upon increasing the molecular core (i.e., 1605 cm^{-1} in **2** and 1614 cm^{-1} in **1**[45]), whereas the same C-C stretching mode located in the innermost benzene ring shifts towards lower frequencies (i.e., 1567 cm^{-1} in **2** and 1562 cm^{-1} in **1**). Thus, the insertion of external triphenylene groups results in an enhancement of the pi-electron delocalization of the central triindole core; note that the displacement of the C-C stretching vibrations towards lower frequencies is associated with an overall relaxation of the structure upon core elongation. On the other hand, the I_{1605}/I_{1567} intensity ratio increases upon enlarging the core of the platform which is also in line with a more efficient π-conjugation in the extended platform **1** when compared to related triindole **2**.

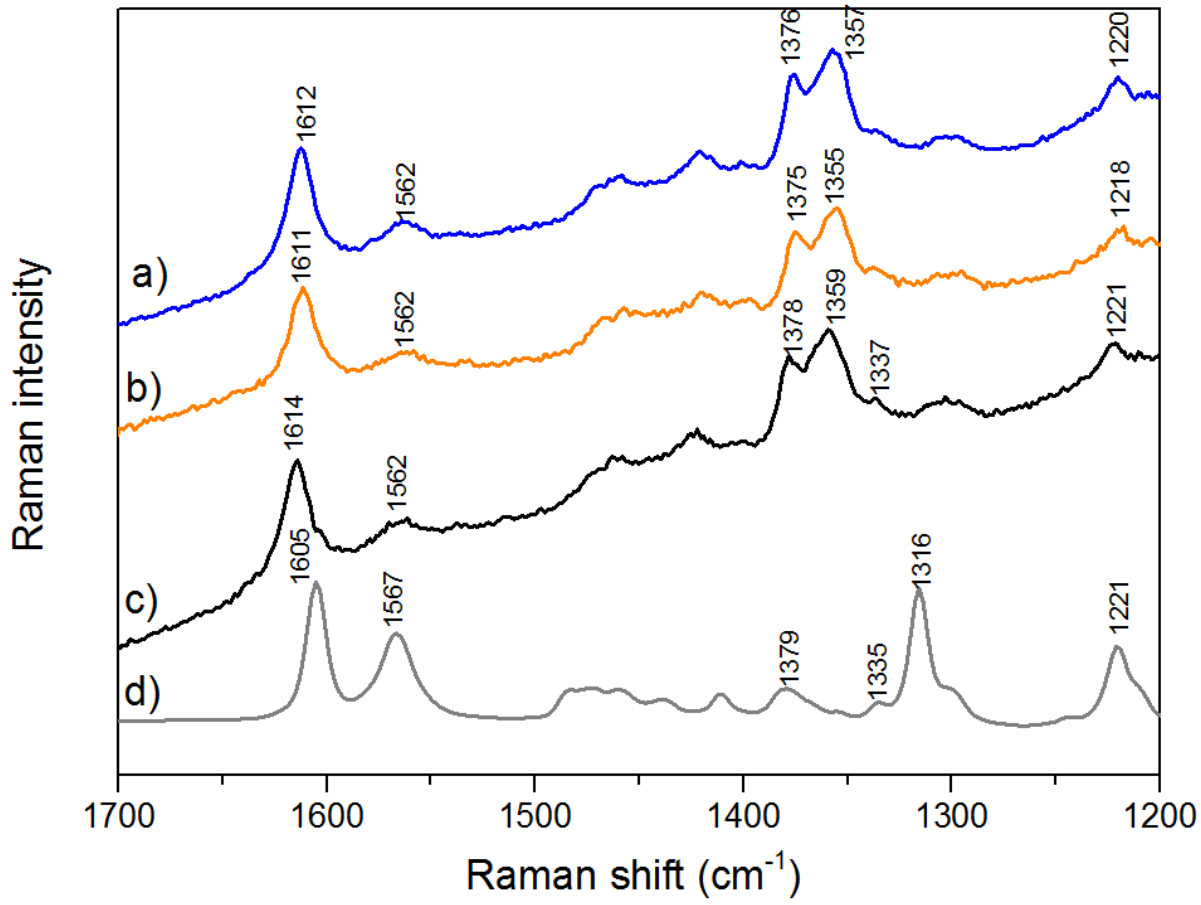

Figure 2. Raman spectra for drop-casted thin films of extended triindole **1** in SiO_2 (a) and gold (b) surfaces and as a bulk (c). The Raman spectra of N-dodecyl triindole **2** as a bulk (d) is also shown for comparison.

The extended triindole platform shows a high tendency to self-assemble in solution as determined by a ^{1}H-NMR study at variable temperature. In chloroform solution, the ^{1}H-NMR spectra of compound **1** are concentration dependent, with several aromatic proton signals of the core shifting upfield with increasing the concentration (see Figure 3). This effect has been well documented as symptomatic of aromatic interactions and reflects the magnetic anisotropy that an aromatic system exerts on a proton in its close vicinity.[46,47] Study of self-aggregation by NMR provides important information on the geometry of aggregates. In this particular case, the central

triindole protons and the protons labeled as *a* and *b* in the triphenylene unit are the most affected, while those placed in the fiord region (labeled as *d*) remain nearly constant. A clear pronounced upfield effect is also observed for the α–CH_2 (labeled as *m*) proton signals of the *N*-dodecyl chains. The different extent of shielding effects observed in the different proton signals suggests an alternated arrangement in which each molecule is rotated by 60º with respect to the next molecular unit. Such arrangement would place *Hd* and *Hd´* protons out of the shielding cone of the aromatic system, thus explaining their poor shifting.

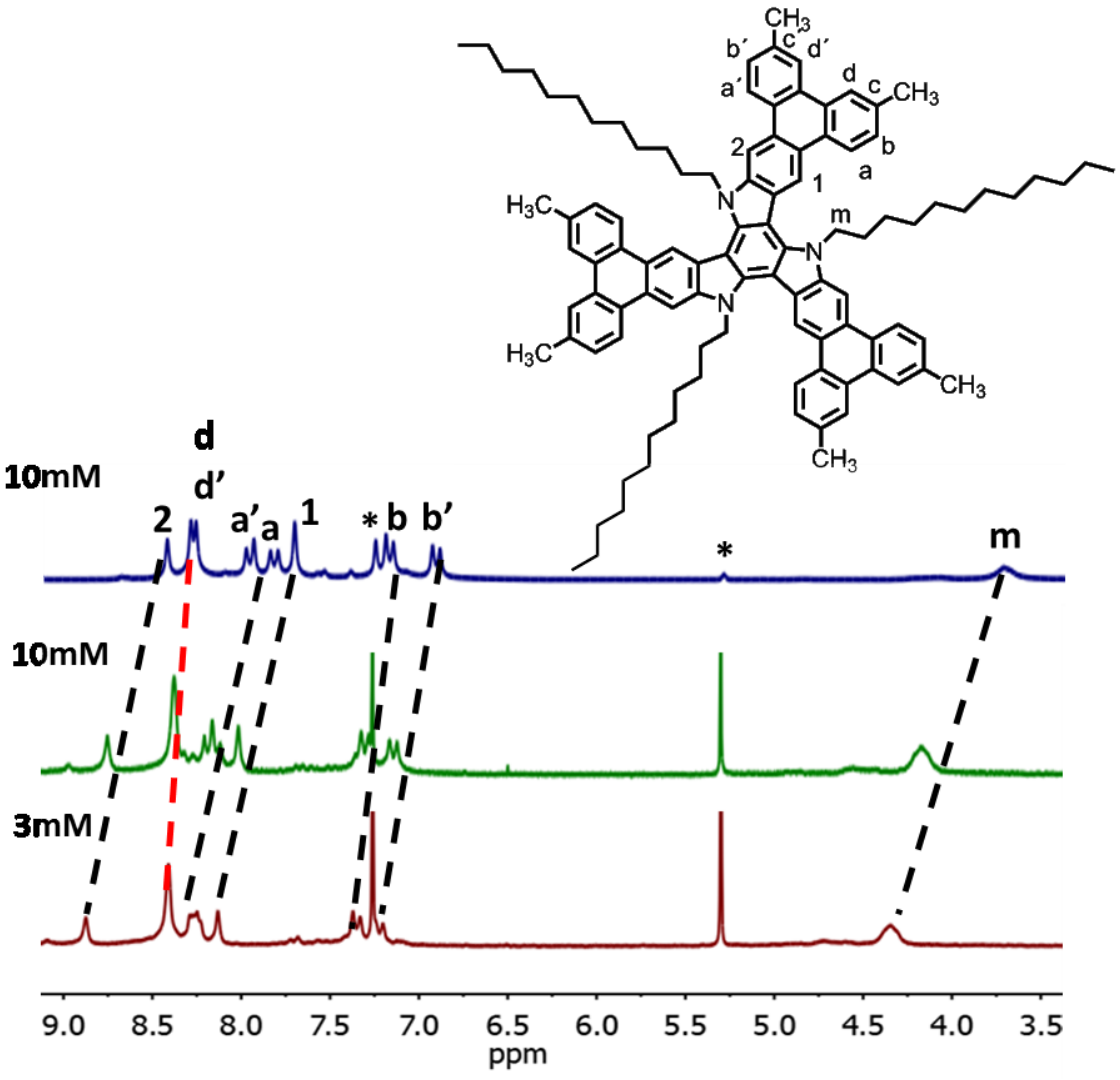

Figure 3.Variation of the aromatic and methylenic ^{1}H-NMR signals of compound **1** upon varying the concentration. Dashed lines have been added to facilitate the visualization of the different shielding effects observed in the different proton signal (those less affected, in red). Signals assigned to $CHCl_3$ and residual CH_2Cl_2 solvent are marked with asterisks.

Charge mobility measurements were performed initially by the Space Charge Limited Current (SCLC) method on samples sandwiched between two electrodes. This method has been widely used to measure the mobility of different triindole-based derivatives[20-23] and other discotic mesogens.[29,48] It should be noted that this technique measures the bulk mobility and it is very sensitive to the degree of macroscopic orientational order (as it requires a conduction channel perpendicular to the electrodes) and to the effectiveness of charge injection at the electrodes.

In a current/voltage measurement, at low fields the observed current is ohmic, depending linearly on the field, while at higher fields the number of injected charges starts to be non-negligible and a space-charge field is present, with the current following the Mott-Gurney equation:

$$J = \frac{9}{8}\varepsilon_0\varepsilon_r\mu\frac{V^2}{d^3} \qquad (1)$$

where J is the measured current density, ε_0 is the free space permittivity, μ is the charge mobility, V is the applied voltage, ε_r is the relative dielectric constant of the material and d is the thickness of the compound layer in the device. From the equation, since the relative dielectric constant ε_r and the sample thickness can be easily measured, it is possible to obtain the mobility. By using this method, in order to extract meaningful information from experiments, materials have to be sandwiched between two electrodes which are chosen in such a way that an ohmic contact is obtained either with the HOMO level of the molecular semiconductor or with its LUMO level. In

the first case hole mobility can be measured, while electron mobility is extracted in the second case.

Considering that triindoles are well-known hole conductors, in order to obtain an ohmic contact we selected gold as the positive electrode because its work function W(Au) = -5.1 eV matches the HOMO value of **1** (- 5.12 eV). As a counter-electrode we used ITO because its work function W(ITO) ~ - 4.6 eV is much lower than the estimated LUMO energy of **1** (-2.84 eV) and because, being transparent allows us to check the orientation of the liquid crystal by Optical Microscopy. In this particular case, Polarizing Optical Microscopy indicates that the sample is partially aligned (see Figure S1): the alignment of the mesophase director (i.e. of the columnar axes) is not uniform within the samples, but domains of different size and orientation are observed. Only some areas the samples show the homeotropic alignment (director along the normal to the electrodes) that, given the geometry of the SCLC samples, allows the measurement of the component of the charge mobility tensor with the highest magnitude. Our sample preparation method allows independent measurements in several different areas of the same sample and the mobility values reported in the following were obtained only in the areas with good homeotropic alignment. In other areas, with non-homeotropic alignment or with smaller domains of various orientations, only an ohmic current regime with much smaller currents (three to five orders of magnitude lower) was recorded, preventing the measurement of charge mobility. Figure 4 shows a typical J/V curve, acquired by connecting the positive pole to the Au electrode and the negative pole to the ITO. As it can be observed, the shift from the ohmic to the SCLC regime is quite clear.[49] Different samples showed similar behavior and the resulting average value of hole mobility is 0.65 ± 0.15 $cm^2V^{-1}s^{-1}$.

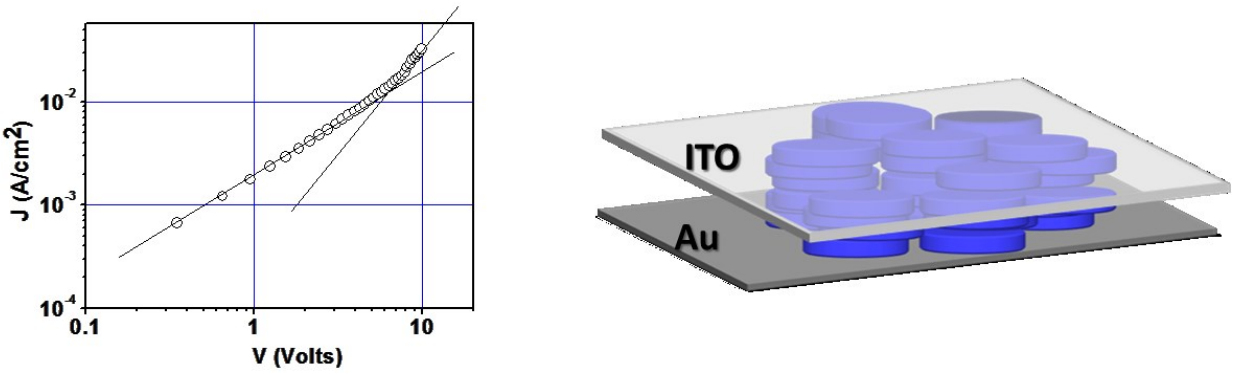

Figure 4. Current vs. Applied voltage for a 22 μm thick sample of **1**. The two continuous lines, with slopes 1 and 2, are a guide to the eye and they respectively represent ideal ohmic and SCLC regimes of the current as a function of applied voltage.

As a complementary method, we have measured the charge mobility of this semiconducting mesogen in a field effect transistor device. In this technique charge transport relies on the first few layers of molecules and its performance depends strongly on the molecular orientation of the semiconductor at the dielectric-semiconductor interface. Thin-film transistors were fabricated in a bottom gate, top contact configuration by drop-casting a chloroform solution of **1** on HMDS-functionalized Si/SiO_2 substrate, followed by evaporation of gold source/drain electrodes through a shadow mask. Charge transport evaluation was carried out *via* analysis of the OFET current-voltage response in the saturation regime with the hypothesis of conventional transistors theory, following eqn:

$$I_D = \frac{WC_{ox}\mu}{2L}(V_G - V_{th})^2 \qquad (2)$$

Where W and L are the channel width and length, respectively, C_{ox} is the capacitance per unit area of the dielectric layer, μ is the hole mobility and V_{th} is the threshold voltage. Figure 5 shows

both the transfer (measured at a fixed source-drain voltage of -80 V) and output curves of the studied semiconductor. The output curves of **1** were measured at gate voltages from 0 to -80 V in intervals of -20 V, the negative working gate voltage region indicating that **1** is a hole transporting semiconductor (Figure 5b). The fundamental parameters dictating the transistor performance were extracted from the transfer plot shown in Figure 5a following equation 2. A hole mobility of 1.01×10^{-4} $cm^2V^{-1}s^{-1}$ with a threshold voltage close to -2 V could be determined with this technique. An on/off ratio of only 7 was estimated for this transistor, which can be ascribed to the low mobility measured in this configuration that results in a low on-current and a relatively large off-current probably due to some oxidative doping.

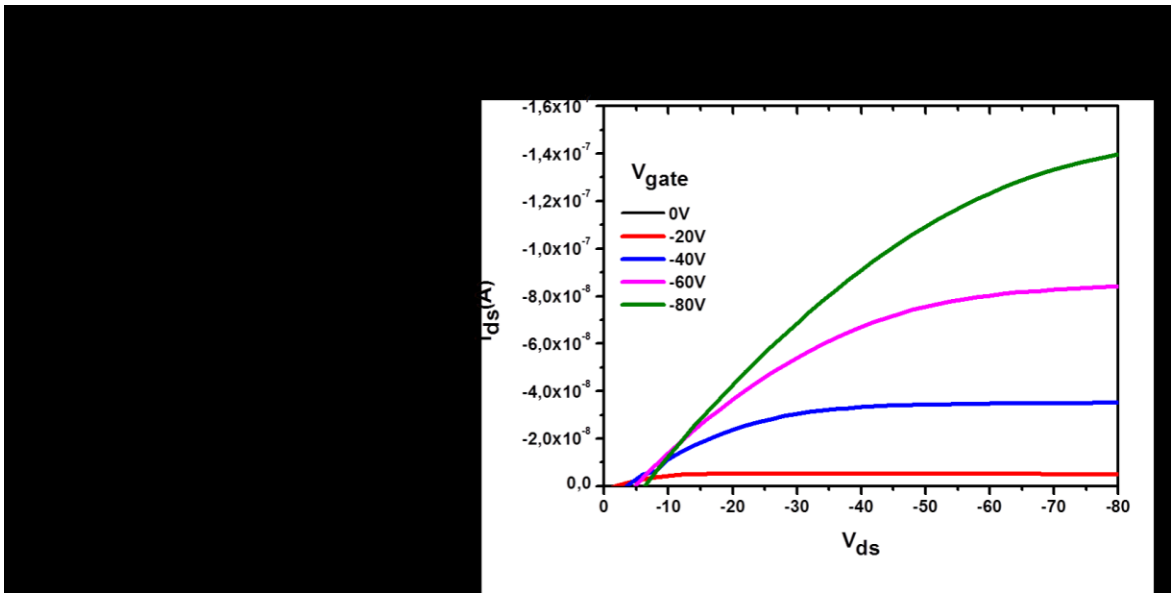

Figure 5. a) Transfer characteristics of **1** measured at a source-drain voltage of -80V. Linear plot of the drain current versus the gate voltage. b) Characteristic transistor curves of **1** measured at gate voltages from 0 to -80V in intervals of 20V.

Note that due to the uniaxial conduction found in discotic liquid crystals it is common to observe charge transport differences of up to more than 5 orders of magnitude when comparing

carrier mobilities along different directions, performed by a different or even by the same technique.[50,51] In order to shed light on the origin of the lower OFET charge mobility when compared to the SCLC mobility, we investigated the molecular orientation at the bottom interfaces of thin films of compound **1** by Surface Enhanced Raman Scattering (SERS). SERS is a very useful technique for the characterization of molecular features near the surface providing valuable information of the interfacial layer in thin films[52,53] as it allows for greatly enhanced Raman scattering from molecules that have been adsorbed onto specially prepared metal surfaces.[54]This surface enhancement (*i.e.*, the surface signal overwhelms the bulk signal) is a combination of a local enhancement of the electromagnetic field and contributions from the chemical interactions between the molecules and the metal surface. We carried out Raman measurements on drop-casted and spin-coated films of triindole **1** prepared on gold and SiO_2 surfaces. Neither Raman enhancement of selected peaks nor appearance of new peaks is observed when comparing the film spectra of **1** on SiO_2 and on gold surfaces (see Figure 2). Similar results are found for the films prepared by either drop-casting or spin-coating (see Supporting Information). Note that normal modes involving vibrations associated with a component of the polarizability tensor which is normal to the surface should be selectively enhanced due to the SERS effect. In the case of an "edge-on orientation", these normal modes would be the ones associated with a component of the polarizability tensor along the molecular axis, such as the ones recorded at 1614 and 1562 cm^{-1} (see corresponding eigenvectors in Supporting information). However, no changes in Raman intensity are recorded for films deposited on both substrates (SiO_2 and gold), thus suggesting that compound **1** takes a "face-on" orientation with respect to the substrate, which would hamper transport parallel to the dielectric as required in OFETs. This is consistent with the decrease in the mobilities values obtained when

comparing the thin-film transistor devices and SCLC measurements in a diode-like structure where, on the contrary, the charge-transport occurs through cofacially overlapped molecules.

In order to analyze in more detail the charge-transport parameters impacting the charge mobility of **1** at the molecular level we have carried out DFT calculations of the reorganization energy and electronic coupling of this π-extended core.

The charge-transport properties of a particular system is connected to the interplay between charge localization effects due to electron-phonon coupling and a charge delocalization effect due to the electronic coupling. The reorganization energy, λ, measures the strength of the so-called local electron-phonon coupling,[55] the smaller λ, the larger the expected charge mobility. Here we focus on the intramolecular reorganization energy associated with hole transfer (λ_h) that reflects the geometric changes needed to accommodate charge. As seen in Figure 6a, enlarging the size of the central core by attaching external triphenylene groups results in smaller λ_h values (*i.e.*, λ_h decrease by 84 meV[40] when comparing **1** and **2** as expected with increasingly larger conjugated backbones). This is consistent with the small participation of the external triphenylene groups in the geometrical relaxation upon oxidation which is in line with their minimal contribution to the HOMO wave functions (*i.e.*, for both extended **1** and related triindole **2,** HOMO wave functions are mainly localized in the central triindole core, see Figure 6b). It is interesting to note that the calculated λ_h value in triphenylene-extended triindole (i.e., 147 meV in **1**) is even smaller than that calculated for benchmarking hole-transport materials such as rubrene (159 meV).[56]

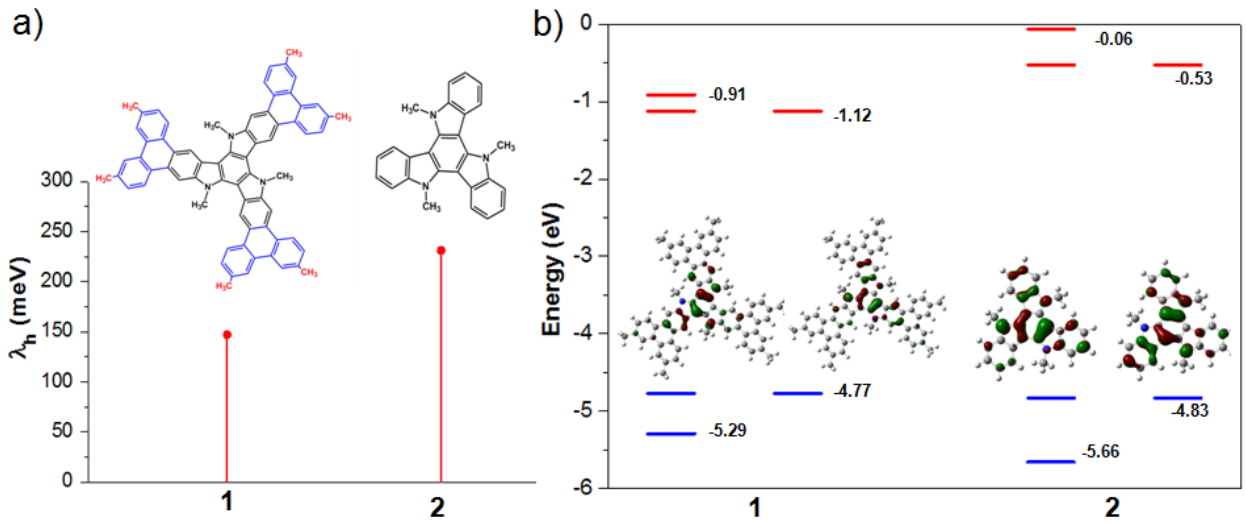

Figure 6. a) DFT-calculated reorganization energy values for holes (λ_h) for triphenylene-extended triindole **1** and related triindole **2** at the B3LYP/6-31G** level. b) B3LYP/6-31G** molecular orbital energies and topologies for both derivatives.

The electronic coupling is defined by the transfer integral and is highly sensitive to the relative position of interacting units and the intermolecular distance between them. A cofacial dimer in a staggered fashion, with a rotation angle of 60º between the disks and an intermolecular distance of 3.8 Å have been considered here for the calculation of the transfer integral (see Figure 7). We have chosen this geometry for the adjacent molecules in view of the aggregation tendency of this compound as deduced from variable concentration NMR studies (see above) and the high propensity of triindoles to adopt this arrangement both in single crystals and solution[57-59] even though probably the rotation by 60 degrees between neighboring molecules is not the optimum arrangement for the transfer of a charge carrier. The intermolecular distance of 3.8 Å have been chosen considering the intrastack periodic distance determined experimentally by X-Ray diffraction measurements of the mesophase. The calculated hole transfer integral for this dimer is found to be -52 meV. Therefore, the HOMO electronic coupling

remains moderate for staggered dimers (60º rotated) highlighting the crucial role played by wave function overlap in the central core of the triindole platforms. Note that slightly larger values are obtained for an equivalent dimer made of two triindole molecules (see Supporting Information). The calculated reorganization energy in the π–extended model is much larger than the electronic coupling, this result suggests that charge localization takes place and transport is expected to occur via a charge-hopping mechanism. In this case, the hopping rate can be estimated in the context of the semi-classical Marcus theory as[60]

$$k_{ET} = t^2 \sqrt{\frac{\pi}{\hbar^2 k_B T \lambda}} exp\left(-\frac{\lambda}{4k_B T}\right) \qquad (3)$$

where λ is the reorganization energy, *t* the transfer integral, k_B the Boltzman constant, T the temperature and ħ the Planck constant.

At high temperature, the mobility can be expressed as[61]

$$\mu = \frac{qd^2}{k_B T} k_{ET} \qquad (4)$$

where d is the intermolecular distance between the molecules.

Rough estimates of the transfer rates and mobilities can be made by injecting in eqs. 3 and 4 the calculated charge transport parameters for the π-extended aromatic compound **1**. It is remarkable, that in spite of all the approximations made, the intrisic hole mobility calculated for compound **1** (0.80 $cm^2V^{-1}s^{-1}$) is only slightly higher than the experimental value obtained by SCLC measurements (0.65 $cm^2V^{-1}s^{-1}$), considering that mobility can be strongly influenced by defects and fluctuations in the columns. Note that although the semiclassical approximation, Marcus theory has been used extensively to study 1D discotic liquid crystals[62] and other columnar systems where a very good agreement between theory and experiments have been

achieved, a more detailed atomistic molecular dynamic simulation would be required, to account for the ordering of the molecules in the columnar arrangement.[64]

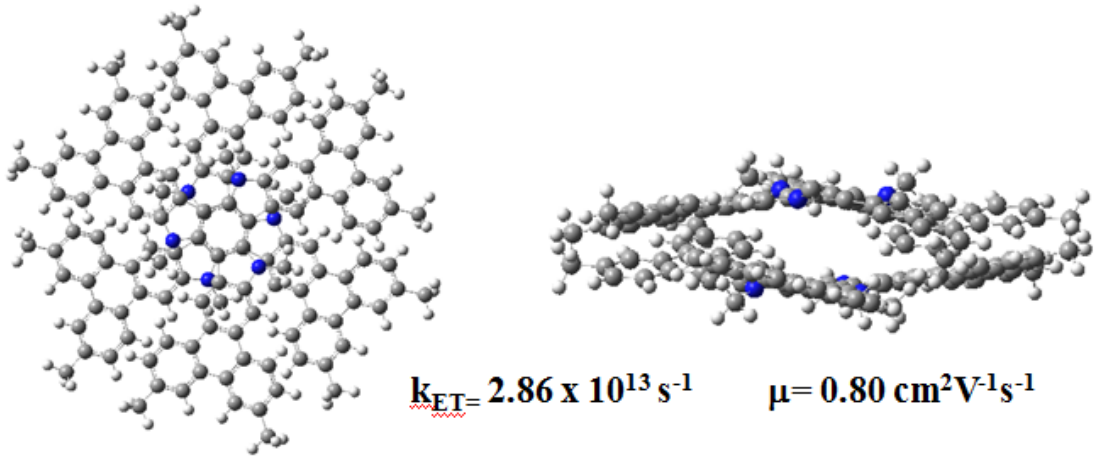

Figure 7. Top and lateral views of a cofacial dimer of **2** in a staggered fashion, with a rotation angle of 60º between the disks and an intermolecular distance of 3.8 Å. The transfer rates (k_{ET}) and mobilities (μ) calculated for the model dimer are also shown.

Conclusion

In conclusion we have investigated the electrical properties of a discotic liquid crystal based on a π-extended aromatic compound containing structural characteristics of both triphenylene and triindole using two complementary methods: space-charge limited current (SCLC) measurements in a diode-like structure and field effect mobility measurements in a thin film transistor device. The mobility found on a diode type device is far higher than that determined on thin film transistors, which can be rationalized by the tendency of these large π-conjugated molecules to

align on metal and oxide surfaces with their extended core parallel to the substrate as demonstrated by SERS. However the observation of field effect behavior in a discotic liquid crystal processed by simple drop-casting suggests that the strategy of lowering the conducting/isolating ratio in discotic mesogens successfully decreases the alignment dependence of charge transport characteristic of these self-assembling materials by enabling hopping between neighboring columns. The hole-mobility of this material theoretically predicted via a charge-hopping mechanism is in very good agreement with the experimental values determined at the space-charge limited current (SCLC) regime. The high mobility found for this compound in a diode type configuration render it a good candidate for OPVs and OLEDs devices.

ASSOCIATED CONTENT

Supporting Information.

Additional experimental (details on SCLC measurements and Raman spectra of π-extended triindole **1** as a spin-coated thin film on gold and SiO_2 surfaces) and theoretical data (theoretical Raman spectra and vibrational eigenvectors associated with the most outstanding Raman features of extended triindole **1**; calculated Transfer Integrals for the HOMO Levels in Cofacial Dimers of unsubstituted triindole **2**; cartesian coordinates and energies for all energy-minimized structures). This material is available free of charge via the Internet at http://pubs.acs.org.

AUTHOR INFORMATION

Corresponding Author

* E-mail: bgl@icmm.csic.es, Phone: (+34) 91-3349031, Fax: (+34) 91-3720623

ACKNOWLEDGMENT

This work was funded by the Spanish Government MINECO CTQ2013-40562-R grants; and the Comunidad de Madrid S2013/MIT-2740 (PHAMA_2.0). AG thanks support from the ELIOTROPO project (PON03PE_00092_2). RT was supported by MIUR under the PRIN 2012JHFYMC project. The work at the University of Málaga was supported by MINECO (project reference CTQ2015-66897) and Junta de Andalucía (P09-FQM-4708). M.C.R.D. and R.P.O. thank the MICINN for a "Ramon y Cajal" Research contract". We acknowledge stimulating discussions related with the charge-transport properties with Professor Gjergji Sini.

REFERENCES

[1] *Organic Electronics: Materials, Manufacturing and Applications*; Klauk, H., Ed.; Wiley-VCH: Weinheim, 2006.

[2] *Organic Electronics: More Materials and Applications*; Klauk, H., Ed.; Wiley- VCH: Weinheim, 2012.

[3] *Chemistry of Discotic Liquid Crystals: From Monomers to Polymers*; Kumar, S. Ed.; CRC Press, Taylor & Francis: Boca Raton, 2011.

[4] Laschat,S.; Baro, A.; Steinke, N.; Giesselmann, F.; Hagele, C.; Scalia, G.; Judele, R.; Kapatsina, E.; Sauer, S.; Schreivogel, A. Discotic Liquid Crystals: From Tailor-Made Synthesis to Plastic Electronics *Angew. Chem. Int. Ed.* **2007**, 46, 4832-4887.

[5] Wöhrle, T. ; Wurzbach, I. ; Kirres, J.; Kostidou, A.; Kapernaum, N.; Litterscheidt, J.; Haenle, J. C.; Staffeld, P.; Baro, A.; Giesselmann, F.; Laschat, S. Discotic Liquid Crystals *Chem. Rev.* **2016**, 116, 1139–1241.

[6] Ruiz, C.; García-Frutos, E. M.; Hennrich, G.; Gómez-Lor, B. Organic Semiconductors toward Electronic Devices: High Mobility and Easy Processability *J. Phys. Chem. Lett.* **2012**, 3, 1428-1436.

[7] Sergeyev, S. Pisula, W.; Geerts, Y. H. Discotic Liquid Crystals: a New Generation of Organic Semiconductors. *Chem. Soc. Rev.* **2007**, 36, 1902-1929.

[8] Pisula, W.; Zorn, M.; Chang, J. Y.; Müllen, H.; Zentel, R. Liquid Crystalline Ordering and Charge Transport in Semiconducting Materials *Macromol. Rapid Commun.* **2009**, 30, 1179-1202.

[9] O´Neill, M.; Kelly, S. M. Ordered Materials for Organic Electronics and Photonics *Adv. Mater.* **2011**, 23, 566-584.

[10] Kaafarani, B. R. Discotic Liquid Crystals for Opto-Electronic Applications. *Chem. Mater.* **2011**, 23, 378-396.

[11] Eccher, J.; Zajaczkowski, W.; Faria, G. C.; Bock, H.; von Seggern, H.; Pisula, W.; Bechtold, I. H. Thermal Evaporation versus Spin-Coating: Electrical Performance in Columnar Liquid Crystal OLEDs. *ACS Appl. Mater. Interfaces* **2015**, 7, 16374-16381.

[12] Shklyarevskiy, I.O.; Jonkheijm, P.; Stutzmann, N.; Wasserberg, D.; Wondergem, H. J.; Christianen, P. C. M.; Schenning, A. P. H. J.; de Leeuw,D. M.; Tomovic, Z.; Wu, J.; Müllen, K.; Maan, J. C. High Anisotropy of the Field-Effect Transistor Mobility in Magnetically Aligned Discotic Liquid-Crystalline Semiconductors. *J. Am. Chem. Soc*., **2005**, 127, 16233-16237.

[13] Miyajima, D.; Araoka, F.; Takezoe, H.; Kim, J.; Kato, K.; Takata, M.; Aida, T. Electric-Field-Responsive Handle for Large-Area Orientation of Discotic Liquid-Crystalline Molecules in Millimeter-Thick Films. *Angew. Chem. Int. Ed*., **2011**, 50, 7865-7869.

[14] Hu, N.; Shao, R.; Shen, Y.; Chen, D.; Clark, N. A.; Walba, D. M. An Electric-Field-Responsive Discotic Liquid-Crystalline Hexa-peri-Hexabenzocoronene/Oligothiophene Hybrid. *Adv. Mater.*, **2014**, 26, 2066-2071.

[15] Kim, H. -S.; Choi, S. -M.; Lee,J. -H.; Busch, P.; Koza,S. J.; Verploegen, E. A.; Pate, B. D. Uniaxially Oriented, Highly Ordered, Large Area Columnar Superstructures of Discotic Supramolecules using Magnetic Field and Surface Interactions. *Adv. Mater.* **2008**, 20*,* 1105-1109.

[16] Bramble, J. P.; Tate, D. J.; Revill, D. J.; Sheikh, K. H.; Henderson, J. R.; Liu, F.; Zeng, X.; Ungar, G.; Bushby, R. J.; Evans, S. D. Planar Alignment of Columnar Discotic Liquid Crystals by Isotropic Phase Dewetting on Chemically Patterned Surfaces. *Adv. Funct. Mater.* **2010**, 20, 914-920.

[17] Kajitani, T.; Suna, Y.; Kosaka, A.; Osawa, T.; Fujikawa, S.; Takata, M.; Fukushima, T.; Aida, T. o-Phenylene Octamers as Surface Modifiers for Homeotropic Columnar Ordering of Discotic Liquid Crystals. *J. Am. Chem. Soc.* **2013**, 135, 14564-14567.

[18] Mouthuy,P. -O.; Melinte, S.; Geerts, Y. H.; Jonas, A. M. Uniaxial Alignment of Nanoconfined Columnar Mesophases. *Nano Lett.* **2007**, 7, 2627-2632.

[19] Cattle, J.; Bao, P.; Bramble,J. P.; Bushby,R. J.; Evans, S. D. Lydon, J. E.; Tate, D. J. Controlled Planar Alignment of Discotic Liquid Crystals in Microchannels Made Using SU8 Photoresist. *Adv. Funct. Mater.* **2013**, 23, 5997-6006.

[20] García-Frutos,E. M.; Pandey,U. K.; Termine, R.; Omenat, A.; Barberá, J.; Serrano,J. L.; Golemme, A.; Gómez-Lor, B. High Charge Mobility in Discotic Liquid-Crystalline Triindoles: Just a Core Business? *Angew. Chem. Int. Ed*. **2011**, 50, 7399-7402.

[21] Benito-Hernández, A.; Pandey, U. K.; Cavero, E.; Termine, R.; García-Frutos,E. M.; Serrano, J. L.; Golemme, A.; Gómez-Lor, B. High Hole Mobility in Triindole-Based Columnar phases: Removing the Bottleneck of Homogeneous Macroscopic Orientation. *Chem. Mater.* **2013**, 25, 117-121.

[22] Zhao, B.; Liu, B.; Png, R. Q.; Zhang, K.; Lim, K.A.; Luo, J.; Shao, J.; Ho, P.K.H.; Chi, C.; Wu, New Discotic Mesogens Based on Triphenylene-Fused Triazatruxenes: Synthesis, Physical Properties, and Self-Assembly. *J. Chem. Mater.* **2010**, 22, 435-449.

[23] Talarico, M.; Termine, R.; García-Frutos, E. M.; Omenat, A.; Serrano, J. L.; Gómez-Lor, B.; Golemme, A. New Electrode-Friendly Triindole Columnar phases with High Hole Mobility. *Chem. Mater.* **2008**, 20, 6589-6591.

[24] García-Frutos, E. M.; Omenat, A.; Barberá, J.; Serrano, J. L.; Gómez-Lor, B. Highly Ordered π-Extended Discotic Liquid-Crystalline Triindoles. *J. Mater. Chem*. **2011**, 21, 6831-6836.

[25] Rose, A. Space-Charge-Limited Currents in Solids. *Phys. Rev*. **1955**, 97, 1538-1544.

[26] Blom, P. W. M.; de Jong, M. J. M.; van Munster, M. G. Electric-field and temperature dependence of the hole mobility in poly(p-phenylene vinylene). *Phys. Rev. B* **1997**, 55, R656.

[27] Reynaert, J.; Arkhipov, V. I.; Borghs, G.; Heremans, P. Current-voltage characteristics of a tetracene crystal: Space charge or injection limited conductivity? *Appl. Phys. Lett*. **2004**, 85, 603.

[28] Blom, P. W. M.; Tanase, C.; de Leeuw, D. M.; Coehoorn, R. Thickness Scaling of the Space-Charge-Limited Current In Poly(P-Phenylene Vinylene). *Appl. Phys. Lett*. **2005**, 86, 092105.

[29] An, Z.; Yu, J.; Domercq, B.; Jones, S.C.; Barlow, S.; Kippelen, B.; Marder, S. R. Room-Temperature Discotic Liquid-Crystalline Coronene Diimides Exhibiting High Charge-Carrier Mobility in Air. *J. Mater. Chem.* **2009**, 19, 6688-6698.

[30] Newman, C.R.; Frisbie, C. D.; da Silva, D. A.; Brédas, J. L.; Ewback, P. C.; Mann, K. R. Introduction to Organic Thin Film Transistors and Design of n-Channel Organic Semiconductors. *Chem. Mater*. **2004**, 16, 4436-4451.

[31] Braga, D.; Horowitz, C. High-Performance Organic Field-Effect Transistors. *Adv. Mater*. **2009**, 21, 1473-1486

[32] Highest hole and electron mobility values of 2.8 $cm^2V^{-1}s^{-1}$ and 6 $cm^2V^{-1}s^{-1}$ respectively have been reported for semiconducting discotic liquid crystals. See references 21 and 29.

[33] Yoon, M-H.; Kim, C.; Facchetti, A.; Marks, T.J. Gate Dielectric Chemical Structure-Organic Field-Effect Transistor Performance Correlations for Electron, Hole, and Ambipolar Organic Semiconductors. *J. Am. Chem. Soc*. **2006**, 128, 12851-12869.

[34] Usta, H.; Lu, G.; Facchetti, A.; Marks, T.J. Dithienosilole− and Dibenzosilole−Thiophene Copolymers as Semiconductors for Organic Thin-Film Transistors. *J. Am. Chem. Soc.* **2006**, 128, 9034-9035.

[35] Becke, A. D. Density-Functional Thermochemistry. III. The Role of Exact Exchange. *J. Chem. Phys.* **1993**, 98, 5648−5652.

[36] Lee, C. T.; Yang, W. T.; Parr, R. G. Development of the Colle-Salvetti Correlation-Energy Formula into a Functional of the Electron Density. *Phys. Rev. B* **1988**, 37, 785−789.

[37] Harihara, P. C.; Pople, J. A. The Influence of Polarization Functions on Molecular Orbital Hydrogenation Energies. *Theor. Chim. Acta* **1973**, 28, 213−222.

[38] Hehre, W. J.; Ditchfield, R.; Pople, J. A. Self-Consistent Molecular Orbital Methods. XII. Further Extensions of Gaussian-Type Basis Sets for Use in Molecular Orbital Studies of Organic Molecules. *J. Chem. Phys*. **1972**, 56, 2257-2261.

[39] Frisch, M. J.; Trucks, G. W.; Schlegel, H. B.; Scuseria, G. E.; Robb, M. A.; Cheeseman, J. R.; Scalmani, G.; Barone, V.; Mennucci, B.; Petersson, G. A.; Nakatsuji, H.; Caricato, M.; Li, X.; Hratchian, H. P.; Izmaylov, A. F.; Bloino, J.; Zheng, G.; Sonnenberg, J. L.; Hada, M.; Ehara, M.; Toyota, K.; Fukuda, R.; Hasegawa, J.; Ishida, M.; Nakajima, T.; Honda, Y.; Kitao, O.; Nakai, H.; Vreven, T.; Montgomery, J. A., Jr.; Peralta, J. E.; Ogliaro, F.; Bearpark, M.; Heyd, J. J.; Brothers, E.; Kudin, K. N.; Staroverov, V. N.; Kobayashi, R.; Normand, J.; Raghavachari, K.; Rendell, A.; Burant, J. C.; Iyengar, S. S.; Tomasi, J.; Cossi, M.; Rega, N.; Millam, J. M.; Klene, M.; Knox, J. E.; Cross, J. B.; Bakken, V.; Adamo, C.; Jaramillo, J.; Gomperts, R.; Stratmann, R. E.; Yazyev, O.; Austin, A. J.; Cammi, R.; Pomelli, C.; Ochterski, J. W.; Martin, R. L.; Morokuma, K.; Zakrzewski, V. G.; Voth, G. A.; Salvador, P.; Dannenberg, J. J.; Dapprich, S.; Daniels, A. D.; Farkas, Ö.; Foresman, J. B.; Ortiz, J. V.; Cioslowski, J.; Fox, D. J. Gaussian 09, revision C.01; Wallingford, CT, 2009.

[40] Ruiz, C.; García-Frutos, E.M.; Da Silva Filho, D.A.; López Navarrete, J.T.; Ruiz Delgado, M.C.; Gómez-Lor, B. Symmetry Lowering in Triindoles: Impact on the Electronic and Photophysical Properties. *J. Phys. Chem. C*, **2014**, 118, 5470-5477

[41] Brédas, J. L.; Beljonne, D.; Coropceanu, V.; Cornil, J. Charge-Transfer and Energy-Transfer Processes in π-Conjugated Oligomers and Polymers: A Molecular Picture. *Chem. Rev*. **2004**, 104, 4971-5004.

[42] Valeev E. F.; Coropceanu V; da Silva D. A., Salman S., Bredas J. L. Effect of Electronic Polarization on Charge-Transport Parameters in Molecular Organic Semiconductors. *J. Am. Chem. Soc*. **2006**, 128, 9882-9886.

[43] Sini G.; Sears J. S., Bredás J. L. Evaluating the Performance of DFT Functionals in Assessing the Interaction Energy and Ground-State Charge Transfer of Donor/Acceptor Complexes: Tetrathiafulvalene−Tetracyanoquinodimethane (TTF−TCNQ) as a Model Case. *J. Chem. Theory Comput*. **2011**, 7, 602-609.

[44] Wilson, E. B.; Decius, J. C.; Cross, P. C. *Molecular Vibrations. The Theory of Infrared and Raman Vibrational Spectra*; McGraw-Hill: New. York, Toronto, London, 1955.

[45] Ruiz, C.; López Navarrete, J.T.; Ruiz Delgado, M.C.; Gómez-Lor, B. Triindole-Bridge-Triindole Dimers as Models for Two Dimensional Microporous Polymers. *Org. Lett.* **2015**, 17, 2258-2261.

[46] Wu, J.; Fechtenkötter, A.; Gauss, J.; Watson, M. D.; Kastler, M.; Fechtenkötter, C.; Wagner, M.; Müllen, K. Controlled Self-Assembly of Hexa-peri-hexabenzocoronenes in Solution. *J. Am. Chem. Soc.* **2004**, 126, 11311-11321.

[47] García-Frutos, E. M.; Gómez-Lor, B. Synthesis and Self-Association Properties of Functionalized C_3-Symmetric Hexakis(*p*-substituted-phenylethynyl)triindoles. *J. Am. Chem. Soc.* **2008**, 190, 9173-9177.

[48] Cour, I.; Pan, Z.; Lebruin, L. T.; Case, M.A.; Furis, M.; Headrick, R.L. Selective Orientation of Discotic Films by Interface Nucleation. *Org. Electron.* **2012**, 13, 419-424.

[49] Mott, N. F.; Gurney, D. in *Electronic Processes in Ionic Crystals*; Academic Press: New York, 1970.

[50] Eccher, J.; Faria,G. C.; Bock, H.; von Seggern, H.; Bechtold, I. H. Order Induced Charge Carrier Mobility Enhancement in Columnar Liquid Crystal Diodes. *ACS Appl. Mater. Interfaces* **2013**, 5, 11935-11943.

[51] Deibel, C.; Janssen, D.; Heremans, P.; de Cupere, V.; Geerts, Y.; Benkhedir, M.L.; Adriaaenssens, G. J. Charge Transport Properties of a Metal-free Phthalocyanine Discotic Liquid Crystal. *Org. Electron.* 2**006**, *7*, 495-499.

[52] Xu, J.; Diao, Y.; Zhou, D.; Mao, Y.; Giri, G.; Chen, W.; Liu, N.; Mannsfeld, S. C. B.; Xue, G.; Bao, Z. Probing the Interfacial Molecular Packing in TIPS-Pentacene Organic Semiconductors by Surface Enhanced Raman Scattering. *J. Mater. Chem. C* **2014**, *2*, 2985-2991.

[53] Adil, D.; Guha S. Surface-Enhanced Raman Spectroscopic Studies of the Au-Pentacene Interface: A Combined Experimental and Theoretical Investigation. *J. Chem. Phys.* **2013**, 139, 044715.

[54] López-Tocón, I.; Otero, J. C.; Arenas, J. F.; Garcia-Ramos, J. V.; Sánchez-Cortes S. Multicomponent Direct Detection of Polycyclic Aromatic Hydrocarbons by Surface-Enhanced Raman Spectroscopy Using Silver Nanoparticles Functionalized with the Viologen Host Lucigenin. *Anal. Chem*. **2011**, 83, 2518-2525.

[55] Coropceanu, V.; Cornil, J.; da Silva, D. A.; Olivier, Y.; Silbey, R.; Brédas, J. L. Charge Transport in Organic Semiconductors. *Chem. Rev*. **2007**, 107, 926-1076.

[56] Da Silva D. A.; Kim E. G.; Brédas, J. L. Transport Properties in the Rubrene Crystal: Electronic Coupling and Vibrational Reorganization Energy. *Adv. Mater*. **2005**, 17, 1072-1076.

[57] Similar alternated stacking has been observed in aggregates of different triindole derivatives both in solution and in the solid state. See for example references 47, 58 and 59.

[58] García-Frutos, E. M.; Hennrich, G.; Gutierrez, E.; Monge, A.; Gómez-Lor, B. Self-Assembly of C_3-Symmetrical Hexaaryltriindoles Driven by Solvophobic and CH-π Interactions. *J. Org. Chem.* **2010**, 75, 1070-1076.

[59] García-Frutos, E. M.; Gutierrez-Puebla, E.; Monge, M. A.; Ramírez, R; de Andrés, P.; de Andrés, A.; Ramírez, R.; Gómez-Lor, B. Crystal Structure and Charge-Transport Properties Of N-Trimethyltriindole: Novel P-Type Organic Semiconductor Single Crystals. *Org. Electron.* **2009**, 10, 643-652.

[60] Marcus, R. A. Electron Transfer Reactions in Chemistry. Theory and Experiment. *Rev. Mod. Phys.* **1993**, 65, 599-610.

[61] Pope, M.; Swenberg, C. E. *Electronic Processes in Organic Crystals and Polymers*; 2nd Ed.; Oxford University Press: New York, 1999.

[62] Lemaur, V.; da Silva Filho, D. A.; Coropceanu, V.; Lehmann, M.; Geerts, Y.; Piris, J.; Debije, M. G.; van de Craats, A. M.; Senthilkumar, K.; Siebbeles, L. D. A.; Warman, J. M.; Bredás, J.-L.; Cornil, J. Charge Transport Properties in Discotic Liquid Crystals: A Quantum-Chemical Insight into Structure−Property Relationships. *J. Am. Chem. Soc.* **2004**, 126, 3271−3279.

[63] Ruiz Delgado, M.C.; Kim, E.-G.; da Silva Filho, D.A.; Bredas, J.-L. Tuning the Charge-Transport Parameters of Perylene Diimide Single Crystals via End and/or Core Functionalization: A Density Functional Theory Investigation. *J. Am. Chem. Soc.* **2010**, 132, 3375-3387.

[64] Bag, S.; Maingi, V.; Maiti, P.K.; Yelk, J.; Glaser, M. A.; Walba, D. M.; Clark, N. A. Molecular Structure of the discotic liquid crystalline phase of hexa-peri-

hexabenzocoronene/oligothiophene hybrid and their charge transport properties *J. Chem. Phys.* **2015**, 143, 144505.

Table of Contents Graphic

The electrical properties of a triphenylene-fused triindole mesogen have been studied by applying two complementary methods. The mobility found on a diode type device is higher than that determined on thin film transistors, which can be understood by the high tendency of large π-conjugated molecules to deposit on surfaces with their extended core parallel to the substrate